



18th International Conference on Sheet Metal, SHEMET 2019

# Numerical modeling of the 22MnB5 formability at high temperature

Giulia Venturato<sup>a,\*</sup>, Stefania Bruschi<sup>a</sup>, Andrea Ghiotti<sup>a</sup>, Xiao Chen<sup>b</sup>

<sup>a</sup> Department of Industrial Engineering, University of Padova, Via Venezia 1, 35131, Padova, Italy

<sup>b</sup> Ford Research and Advanced Engineering, Ford-Werke GMBH, Henry-Ford-Straße, 1, 50735, Köln, Germany

## Abstract

It has been recognized in automotive sector that the use of hot stamped parts for the automobile body-in-white allows significant weight saving and reduction of CO<sub>2</sub> emissions. The weight reduction is accompanied by high stiffness and increased crashworthiness, which improve the passengers' safety and allow the development of more complex vehicle's design.

In direct hot stamping, the 22MnB5 sheets are heated above the austenitization temperature, and then, formed and quenched in cooled dies by using a minimum cooling rate of 27°C/s in order to obtain the direct martensitic transformation from the initial austenite. To evaluate part feasibility, minimize production cost and improve process robustness in hot stamping, numerical simulations are becoming increasingly important, where data regarding the formability of the material at high temperature plays a central role in the simulation. A survey of the literature shows that the complex aspects of the process have been extensively investigated from an experimental point of view, but limited studies concerning the numerical modeling of the process can be found.

The aim of the present paper is to explore the critical aspects of the numerical modeling in terms of material formability in hot stamping. Numerical simulations of hot Nakajima tests at the critical temperature of 600°C were performed by using explicit numerical method, while experimental tests are carried out in the same condition. The comparison of the numerical results and the experimental data demonstrates the influence that the thermal cycle applied during the experimental tests may have, since it governs the phase transformations that affect the material formability.

© 2018 The Authors. Published by Elsevier B.V.

This is an open access article under the CC BY-NC-ND license (<https://creativecommons.org/licenses/by-nc-nd/4.0/>)

Selection and peer-review under responsibility of the organizing committee of SHEMET 2019.

*Keywords:* Hot Stamping; Formability; 22MnB5; Nakajima Test.

\* Corresponding author. Tel.: +39 048 8276816;  
E-mail address: [giulia.venturato.1@phd.unipd.it](mailto:giulia.venturato.1@phd.unipd.it)

## 1. Introduction

The key point of the direct hot stamping process is to use the phase transformation to increase the mechanical properties of the material. This allows to increase the strength of the parts, while reducing part weight of the body-in-white, the automotive industry has followed the trend in the past years [1].

The success of the hot forming process is given by the control of a large number of parameters. It has been demonstrated that the initial microstructure of the blank can influence the final mechanical properties of the blank after the thermal treatment [2]. A correct heating process generates homogeneous transformation from the initial microstructure to austenite; both the austenitization temperature and the soaking time at that temperature are important to generate the complete transformation of the initial microstructure [3] and their careful combination is fundamental to control the austenitic grain size [4], which then affect the grain size, and the mechanical properties, of the final martensite or bainite-martensite phase. In the same way as the heating and soaking steps, the transfer of the blank from the oven to the forming stage is to be set in order to avoid an excessive cooling of the blank, because the full austenite microstructure is required while the blank is formed: the austenite phase is more formable than martensite or bainite [5, 6] so the final shape can be reached without the failure on the blank. The importance of a fast transfer time lies also in the fact that the mechanical load applied during the forming stage can anticipate the phase transformation. The Continuous Cooling Transformation (CCT) curve of 22MnB5 is largely modified when a strain or a stress is applied to the piece [7, 8] and this means that the deformation can occur when the material microstructure is evolving from austenite to bainite, with a drastic change of the mechanical properties [9]. The strain-stress flow curves demonstrate a change in the slope, with differences in the stress values that can reach over 200 MPa. In these conditions the final piece can present cracks or defects, and the final microstructure can present a mixture of phases, with areas where a large quantity of residual austenite is present, which lead to very weak spots in the part.

Within this framework, the aim of the paper is to investigate the influence of microstructure on the 22MnB5 may have on the material formability when different percentages of austenite and bainite are present, Nakajima tests are taken as references, where the Forming Limit Diagrams (FLD) are obtained from the tests. For this purpose, an accurate thermal calibration was studied and then a series of Nakajima [10] tests were performed. The evolution of microstructure during the test was investigated by means of numerical models developed in the LS-Dyna environment with the material model 244\_UHS\_STEEL. The basic constitutive model of Mat\_244 is based on the model proposed by P. Akerstrom [11, 12]. This material model is mainly suited for hot stamping processes where phase transformations are crucial [13].

## 2. Experimental Procedure

The hot Nakajima tests were performed on 1.5( $\pm$ 0.1) mm thick 22MnB5 sheets. In this study, three geometries were considered according to the ISO 12004-2-2008 standard [14], in order to have the three fundamental points of the FLD. Fig. 1(a) shows the specimens geometry, namely the 30 mm width, to reproduce the uni-axial stress state, the 100 mm width, for the plane stress state, and the 200 mm width, for the axi-symmetric stress state. Fig. 1(b) shows the experimental apparatus used for the hot Nakajima tests. The specimen is fixed between the die (2) and the blank holder (3). The punch (1), equipped with electrical cartridge heaters that allows heating it up to the maximum temperature of 900( $\pm$ 15) °C, is pre-heated at the same temperature at which the test takes place to ensure the specimen deformation under isothermal conditions. For the purposes of this investigation, the punch was kept at a constant temperature of 600( $\pm$ 8) °C, which is also the temperature chosen to perform the Nakajima tests. The blank is heated thanks to an inductor head (6), mounted on a pneumatic system which allows the movement of the copper head both in the horizontal and the vertical directions, to ensure the correct displacement and proper heating of the specimen. Three different inductor heads were used, as shown in Fig. 1(a), to avoid the edge effect, which causes the edges of the specimen to be hotter than the center, creating a preferential area where the fracture initiates. The temperature of the specimen is controlled by a type-K thermocouple (4) spot-welded in different points of the sheet surface, where the deformation occurs. In the same time, the temperature of the punch is controlled by two type-K thermocouples inserted in the punch as close as possible to its hemispherical surface. The strain field in the sheet during deformation was measured using the GOM-ARAMIS<sup>TM</sup> optical system (5), made of two cameras and equipped with a proper

lighting equipment, providing the possibility to display 3D-coordinates of the surface by means of a stochastic pattern previously applied to the sheet metal and capable of resisting high temperature.

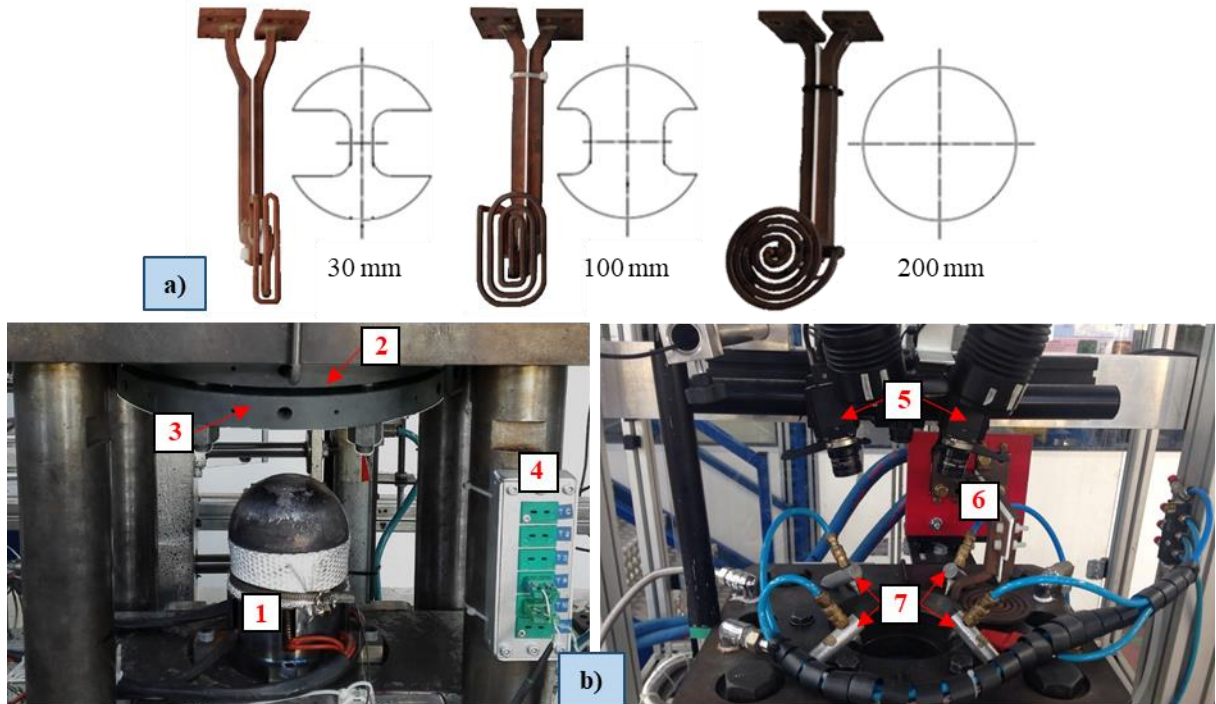


Fig. 1: (a) Specimens geometries and inductor heads used, (b) Nakajima test equipment.

The thermal cycle applied during the tests is shown in Fig. 2(a)-(c): after the heating at  $3(\pm 0.5)$  °C/s from room temperature to the austenitization temperature ( $T_{aust}$ ) 950°C, the specimen was kept at this temperature for 360 s and then cooled down at  $80(\pm 0.5)$  °C/s, by means of the air nozzles (7), to  $600(\pm 8)$  °C. To calibrate the soaking time to be set in the different Nakajima test conditions, the TTT curve at 600°C of 22MnB5 had to be obtained, in order to define the correct thermal cycles that has to be applied. The curve was obtained from a series of test in Gleeble 3800™ simulator equipped with a dilatometer. The specimen was heated up to 950°C, then cooled very fast ( $>100(\pm 0.1)$  °C/s) to  $600(\pm 5)$  °C and it was kept at constant temperature for 360 s. From the data registered with the dilatometer, the curve shown in Fig. 2(d) was obtained.

Then, three different conditions are tested according to the saturation curve shown in Fig 2(d):

1. 100% austenite: after the cooling stage, the specimen is kept at  $600(\pm 8)$  °C for 5 s before the test, as shown in Fig 2(a);
2. 50% austenite – 50% bainite: after the cooling stage, the specimen is kept at  $600(\pm 8)$  °C for 30 s before the test, as shown in Fig 2b and according to the saturation curve shown in Fig 2(d);
3. 100% bainite: after the cooling stage, the specimen is kept at  $600(\pm 8)$  °C for 200 s before the test, as shown in Fig 2(c).

The strain rate selected was  $1 \text{ s}^{-1}$ ; each geometry was tested 5 times and the FLD points here reported are the mean values. The choice to select three different percentage of austenite and bainite in the specimen stands on the understanding of the differences in the formability when the piece is deformed in pure austenite phase, or when the deformation occurs later, when the austenite evolves in a tougher phase, such as bainite.

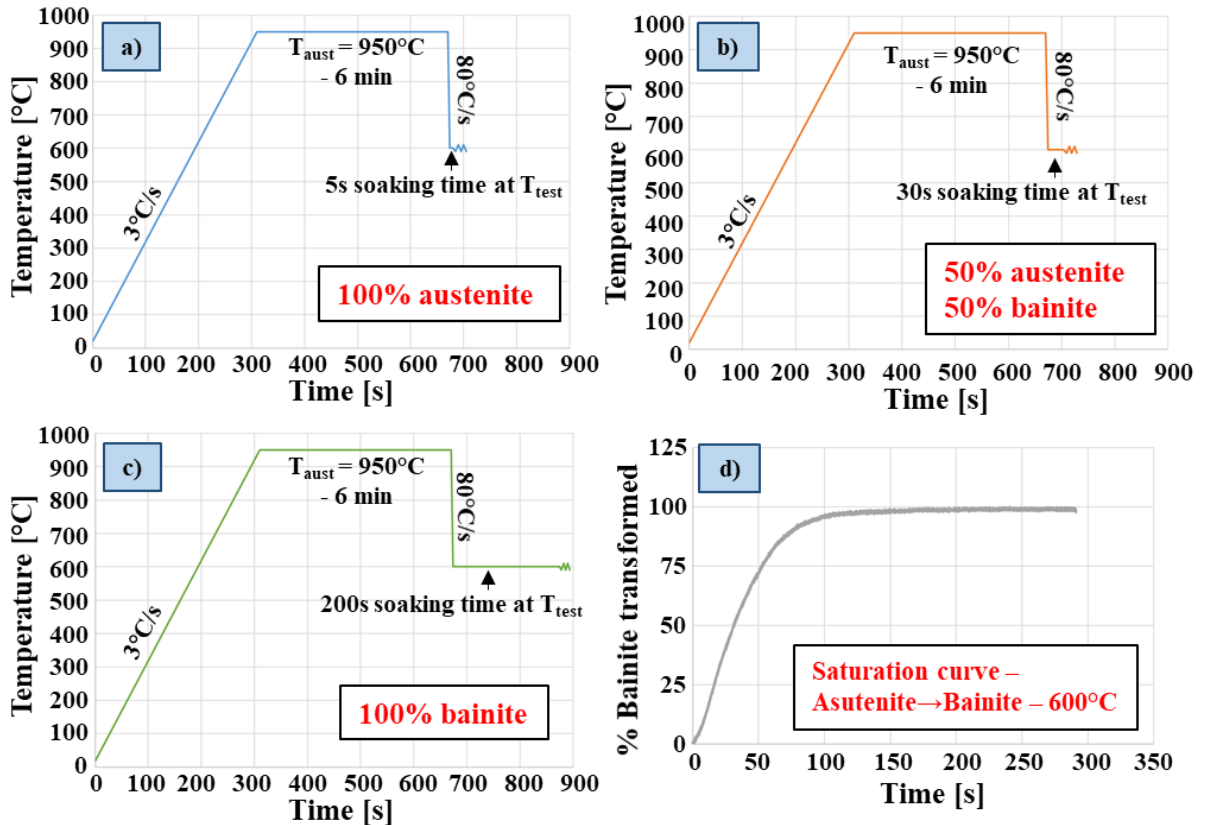


Fig. 2: a) Thermal cycle applied for 100% austenite tests, b) Thermal cycle applied for 50% austenite-50% bainite tests, c) Thermal cycle applied for 100% bainite tests, d) Saturation curve for the transformation of austenite to bainite at 600°C.

### 3. Numerical Model

A series of simulations in the LS-Dyna environment were set reproducing the experimental Nakajima tests carried out in laboratory. The material model MAT\_244\_UHS\_STEEL was used, because it allows the simulation of the phase transformation of the steel according to the model proposed by Akerstrom [11, 12]. The material model allows the implementation of rheology data, such as the Young modulus of the material, the Poisson's ratio, the flow curves of the pure phases involved, and data relatives to the steel, such as the weight percentage of the elements in the steel, the thermal expansion coefficient for austenite and martensite, the latent heat for the decomposition of austenite into ferrite, pearlite, bainite and martensite, the activation energy divided by the universal gas constant for the diffusion reaction of the austenite-ferrite, austenite-pearlite and austenite-bainite reactions, the austenitic grain size and the constant Alpha for the transformation of austenite in martensite, describing the final percentage of martensite after transformation. The start temperature of the phase transformations, namely the ferrite start temperature ( $F_s$ ), the pearlite start temperature ( $P_s$ ), the bainite start temperature ( $B_s$ ), and the martensite start temperature ( $M_s$ ) are obtained according to the chemical composition of the elements in the steel, as shown in Eq. (1) to (4) [13].

$$F_s = 1185 - (203 \times \sqrt{C}) - (15.2 \times Ni) + (44.7 \times Si) + (104 \times V) + (31.5 \times Mo) + (13.1 \times W) - (30 \times Mn) - (11 \times Cr) - (20 \times Cu) + (700 \times P) + (400 \times Al) + (120 \times As) + (400 \times Ti) \quad (1)$$

$$P_s = 996 - (10.7 \times Mn) - (16.9 \times Ni) + (29 \times Si) + (16.9 \times Cr) + (290 \times As) + (6.4 \times W) \quad (2)$$

$$Bs = 910 - (58 \times C) - (35 \times Mn) - (15 \times Ni) - (34 \times Cr) - (41 \times Mo) \quad (3)$$

$$Ms = 812 - (423 \times C) - (30.4 \times Mn) - (17.7 \times Ni) - (12.1 \times Cr) - (7.5 \times Mo) + \\ + (10 \times Co) - (7.5 \times Si) \quad (4)$$

The chemical composition considered was taken from the work of Akerstrom [11] and it is reported in Table 1.

Table 1: Chemical composition of 22MnB5 implemented in the simulation [11].

B %	C %	Cr %	Mn %	Si %	P %
0.003	0.23	0.211	1.25	0.29	0.013

The phase distribution during cooling is calculated by solving the following rate equation for each phase transition

$$\dot{X}_k = g_k(G, C, T_k, Q_k) f_k(X_k) \quad k = 2, 3, 4 \quad (5)$$

Where  $g_k$  is a function, taken from Li et al. [15], dependent on the grain number  $G$ , the chemical composition  $C$ , the temperature  $T$  and the activation energy  $Q$ . The numbers 2, 3, 4 of the  $k$  parameter represents the ferrite, pearlite and bainite phase respectively. Moreover, the function  $f$  is dependent on the actual phase  $X_k = x_k / x_{eq}$

$$f_k(X_k) = X_k^{0.4(X_k-1)} (1-X_k)^{0.4(X_k)} \quad k = 2, 3, 4 \quad (6)$$

The true amount of martensite,  $x_5$ , numbered as 5 representing the martensite phase, is modeled by using the true amount of the austenite left after the bainite phase:

$$x_5 = x_1 [1 - e^{-\alpha(Ms-T)}] \quad (7)$$

Where  $x_1$  is the true amount of austenite left for the reaction (number 1 represents the austenite phase), and  $\alpha$  is a material dependent constant.

According to [16], the best values to represent the friction are 0.25 for the static friction coefficient and 0.1 for the dynamic friction coefficient. The thermal cycle applied in the simulation is the same used in the experimental cycle, in order to represent more accurately the temperature profile distribution in the specimens.

#### 4. Results and Discussion

The formability at fracture of 22MnB5 sheet were determined from the GOM-ARAMISTM data, which describe the experimental strain paths for the three different geometries tested. The final FLD points are the mean values of the major and minor strains at fracture of the five tests repeated for each geometry and conditions, and the error was determined using the standard deviation. The values of the major strain of the FLD points plotted in the diagrams in Fig. 3 are all normalized. Since no fracture criteria is implemented in the numerical simulation, the numerical FLD points were determined considering the stroke at fracture from the experimental tests. In Fig. 3(a) the experimental FLD curves, relative to the three conditions tested, are showed. The higher formability is reached when the specimen is in pure austenite phase, as expected. The formability drops of about the 40% when the tests are performed in pure bainite phase. The curve in the middle, relative to the case 50% austenite and 50% bainite does not stand right in the middle between the others: this can be explained by the fact that during the deformation, the phase transformation continues, even accelerated by the applied strain/stress, so the final percentage of the two phases cannot be maintained exactly balanced. This also affect the experimental error, as described by the error bands in the plot, which represent the standard deviation from the average value. The differences among the three curves stands also in the minor strain values, which is about the 30% lower in the case of pure bainite compared to the other tested conditions. This means that the piece is more likely to fail if the strain path which describes the deformation is too severe. Similar behavior

was seen comparing FLD at different temperatures, where the lower the testing temperature the lower the material formability due to the microstructural modifications [16].

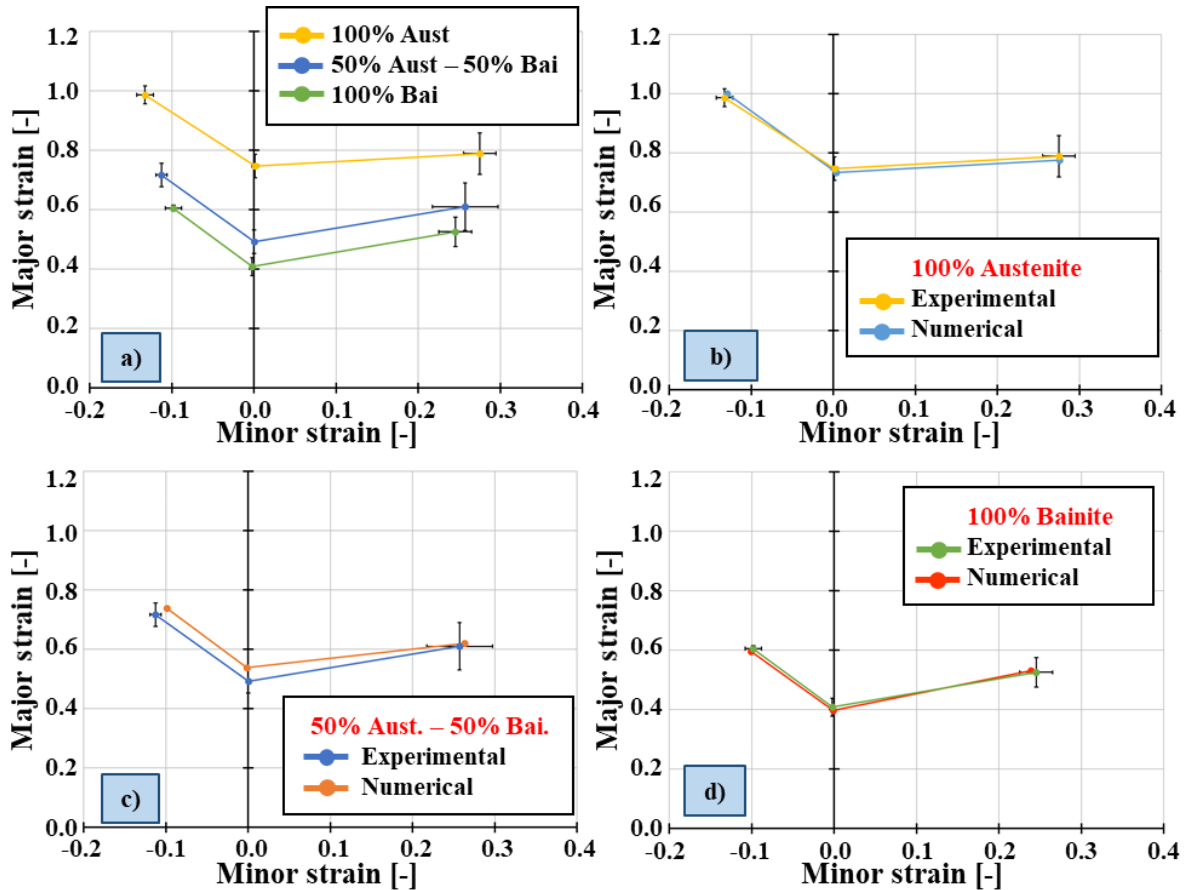


Fig. 3: a) Experimental normalized FLD curves, b) Experimental and numerical FLDs for 100% Austenite, c) Experimental and numerical FLDs for 50% Austenite – 50% Bainite, d) Experimental and numerical FLDs for 100% Bainite.

Fig. 3(b), 3(c) and 3(d) show the comparison between the experimental and the numerical FLDs. The fitting for the cases in pure phase, both austenite and bainite, is good, while the fitting for the mixed phase FLD is less good. This is because the LS-Dyna material model 244 cannot simulate the phase transformation in condition of constant temperature, so the software cannot follow the evolution of the microstructure during the deformation of the specimen.

## 5. Conclusions

In this paper the influence of the microstructure on the formability of 22MnB5 was investigated, both through experimental tests and numerical simulations with following conclusions:

- The formability when the specimen is in pure austenite phase is the highest among the three conditions tested, and this is in agreement with the literature.
- The formability when the specimen is in pure bainite phase is the lowest, in particular the major strain drops of about the 40% and the minor strain drops of about the 30% in respect with the pure austenite case.

- The case representing the 50% Austenite – 50% Bainite does not stand in the middle between the other two curves, because, when the fracture occurs, the phase mixture in the specimen is not exactly 50-50%. This is due to the fact that the microstructural evolution continues during the deformation of the piece.
- The fitting between the experimental data and the numerical data is good for the two cases in which the specimen is in pure phase but, since the material model 244 cannot simulate the phase transformation in isothermal condition, it cannot follow the evolution of the microstructure during the deformation, leading to a less refined fitting.

## Acknowledgments

This research and development project was funded by Ford Motor Company within the Framework of the University Research Project “Advanced CAE method to predict failure and material properties in hot forming” ref. 2014-4050 URP Award.

## References

- [1] 5th Global automotive lightweight materials congress, 2016, available on <http://www.global-automotive-lightweight-materials.com/>
- [2] H. Järvinen, M. Isakov, T. Nyyssönen, M. Järvenpää, P. Peura, “The effect of initial microstructure on the final properties of press hardened 22MnB5 steels”, *Materials Science & Engineering A*, 676 (2016) 109–120.
- [3] N. Li, J. Lin, D.S. Balint, T.A. Dean, “Experimental characterisation of the effects of thermal conditions on austenite formation for hot stamping of boron steel”, *Journal of Materials Processing Technology* 231 (2016) 254–264.
- [4] A. Turetta, A. Ghiotti, S. Bruschi, “Investigation of 22MnB5 Mechanical and Phase Transformation Behaviour at High Temperature”, *II DRG Conference (2007)*, Proceedings, pp. 147–153.
- [5] H. Li, L. He, G. Zhao, L. Zhang, “Constitutive relationships of hot stamping boron steel B1500HS based on the modified Arrhenius and Johnson–Cook model”, *Materials Science & Engineering A*, 580 (2013) 330–348.
- [6] M. F. Novella, G. Venturato, S. Bruschi, A. Ghiotti, “Influence of phase transformation on 22MnB5 mechanical behaviour in hot stamping”, 6<sup>th</sup> International Conference HOT SHEET METAL FORMING of HIGH-PERFORMANCE STEEL CHS 2 June 4-7, 2017, Atlanta, Georgia, USA Proceedings.
- [7] A. Barcellona, D. Palmeri, “Effect of plastic hot deformation on the hardness and continuous cooling transformations of 22MnB5 microalloyed boron steel”, *Metallurgical and Materials Transactions A*, Vol. 40A, MAY 2009, 1160-1174.
- [8] M. Nikravesha, M. Naderi, G.H. Akbari, “Influence of hot plastic deformation and cooling rate on martensite and bainite start temperatures in 22MnB5 steel”, *Materials Science and Engineering A* 540 (2012) 24– 29.
- [9] G. Venturato, M. F. Novella, S. Bruschi, A. Ghiotti, R. Shivpuri, “Effects of phase transformation in hot stamping of 22MnB5 high strength steel”, 17th International Conference on Sheet Metal (2017).
- [10] K. Nakazima, T. Kikuma, K. Asaku, “Study on the formability of steel sheet”, *Yawata Technical Report* 264 (1968).
- [11] P. Akerstrom, M. Oldenburg, “Austenite decomposition during press hardening of a boron steel – computer simulation and test”, *Journal of Material processing technology*, 174 (2006), pp399–406.
- [12] P. Akerstrom, “Numerical implementation of a constitutive model for simulation of hot stamping”, PhD Thesis, Division of Solid Mechanics, Lulea University of technology, Sweden.
- [13] *Ls-Dyna manual 10.0 vol II*, pp 2\_1194-2\_1213.
- [14] Standard ISO 12004-2-2008.
- [15] M.V. Li, D.V. Niebuhr, L.L. Meekisho, and D.G. Atteridge, “A computational model for the prediction of steel hardenability”, *Metallurgical and Materials Transactions B*, 29B(3) (1998), pp 661–672.
- [16] G. Venturato, S. Bruschi, A. Ghiotti, “Influence of temperature and friction on the 22MnB5 formability under hot stamping conditions”, accepted paper for Esaform 2018 conference.